



Discovering novel carbonic anhydrase type IX (CA IX) inhibitors from seven million compounds using virtual screening and *in vitro* analysis

Ramin Ekhteiri Salmas, Murat Senturk, Mine Yurtsever & Serdar Durdagi

To cite this article: Ramin Ekhteiri Salmas, Murat Senturk, Mine Yurtsever & Serdar Durdagi (2016) Discovering novel carbonic anhydrase type IX (CA IX) inhibitors from seven million compounds using virtual screening and *in vitro* analysis, Journal of Enzyme Inhibition and Medicinal Chemistry, 31:3, 425-433, DOI: [10.3109/14756366.2015.1036049](https://doi.org/10.3109/14756366.2015.1036049)

To link to this article: <https://doi.org/10.3109/14756366.2015.1036049>

 View supplementary material 

 Published online: 07 May 2015.

 Submit your article to this journal 

 Article views: 1487

 View related articles 

 View Crossmark data 

 Citing articles: 1 View citing articles 

RESEARCH ARTICLE

Discovering novel carbonic anhydrase type IX (CA IX) inhibitors from seven million compounds using virtual screening and *in vitro* analysis

Ramin Ekhteiari Salmas¹, Murat Senturk², Mine Yurtsever¹, and Serdar Durdagi³

¹Department of Chemistry, İstanbul Technical University, İstanbul, Turkey, ²Department of Chemistry, Ağrı Ibrahim Çeçen University, Ağrı, Turkey, and ³Department of Biophysics, School of Medicine, Bahçeşehir University, İstanbul, Turkey

Abstract

Carbonic anhydrase type IX (CA IX) enzyme is mostly over expressed in different cancer cell lines and tumor tissues. Potent CA IX inhibitors can be effective for adjusting the pH imbalance in tumor cells. In the present work, we represented the successful application of high throughput virtual screening (HTVS) of large dataset from ZINC database included of ~7 million compounds to discover novel inhibitors of CA IX. HTVS and molecular docking were performed using consequence Glide/standard precision (SP), extra precision (XP) and induced fit docking (IFD) molecular docking protocols. For each compound, docking code calculates a set of low-energy poses and then exhaustively scans the binding pocket of the target with small compounds. Novel CA IX inhibitor candidates were suggested based on molecular modeling studies and a few of them were tested using *in vitro* analysis. These compounds were determined as good inhibitors against human CA IX target with K_i in the range of 0.85–1.58 μM . In order to predict the pharmaceutical properties of the selected compounds, ADME (absorption, distribution, metabolism and excretion) analysis was also carried out.

Introduction

Carbonic anhydrase (CA) family includes different isomers that display different level of enzyme activity and kinetic characteristics^{1–11}. Only two of the CA isomers are distinguished as targets that are related to cancer: CA IX and CA XII¹². While CA IX is commonly represented in a narrow number of ordinary tissues, its over expression is identified on solid tumors, where it is always connected with the hypoxic phenotype, mediated by the transcription factor HIF-1¹³. Over expression of CA IX is mostly affiliated with a weak responsiveness to classical chemotherapy¹⁴. CA IX has been the subject of several studies as an enzyme responsible for the pH adjustment of tumor cells, as well as for the cell reproduction and cell adhesion^{15,16}. It is an important target for cancer diagnostics and therapy¹⁷. CA IX has an N-terminal domain, an extracellular CA catalytic domain, a trans-membrane (TM) helical domain and a short intra-cytoplasmic tail. The first domain plays an important role in the protein-mediated cell adhesion events. The catalytic domain catalyzes the reversible hydration of CO_2 , thus it contributes to pH regulation¹⁸. In this work, a large ligand database (~7 million) from ZINC database is used to detect novel CA IX inhibitors using high throughput virtual screening (HTVS) approach. A few proposed compounds based on virtual screening analysis are then tested by the *in vitro* and experimental data confirmed simulation results. Absorption,

Keywords

ADME, carbonic anhydrase, CA IX inhibitors, molecular docking, virtual screening

History

Received 4 November 2014
Revised 24 March 2015
Accepted 27 March 2015
Published online 7 May 2015

distribution, metabolism and excretion (ADME) profiles of studied compounds are also predicted using molecular modeling techniques.

Methods

Structural preparation of enzyme

The crystal structure of carbonic anhydrase¹⁹ IX (CA IX) (PDB ID: 3IAI) has been taken from the Protein Data Bank²⁰. This structure is a dimer, which involves two identical inhibitors (Figure 1) inside the binding sites. In this work only one chain is used for docking simulations. Hydrogen atoms were added using Protein Preparation Wizard²¹ integrated in the Maestro molecular modeling Suite. The disulfide bond between Cys23 and Cys203 was constrained utilizing the patch DISU command during preparation²². The PROPKA^{23–25} program is used to locate protonation states at the physiological pH of 7.4. Hydrogen atoms were then relaxed using the energy minimization.

MD simulations protocol

In order to relax the side chains of the CA IX complex, 10 ns MD simulations was performed before the docking simulations. Ligand–protein complex was hydrated with explicit water molecules using TIP3P water models, and neutralized by 0.15 M KCl using VMD (Visual Molecular Dynamics)²⁶ program. MD simulations were then carried out using the parallel MD software²⁷ NAMD 2.9 with CHARMM36 force-field parameters²⁸. SHAKE algorithm was used to restrain the hydrogen atoms. Langevin piston method with Langevin thermostat was

Address for correspondence: Serdar Durdagi, Associate Professor, Department of Biophysics, School of Medicine, Bahçeşehir University (BAU), İstanbul, Turkey. Tel: +90-216-579-8217. E-mail: serdar.durdagi@med.bahcesehir.edu.tr

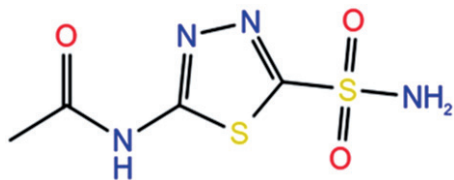


Figure 1. Chemical structure of acetazolamide (AZM) exists in each monomer.

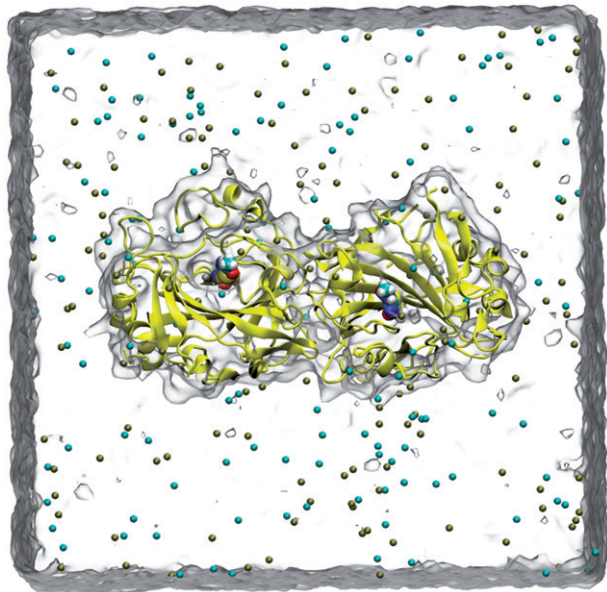


Figure 2. A snapshot picture taken from the simulation box: Protein (CA IX-dimer in yellow, inhibitor (inside the protein), water (as quick surface) and K^+ , Cl^- ions (cyan and brown colored spheres).

used to maintain constant temperature at 310 K and at a constant pressure of 1 atm during simulations. Periodic Boundary Conditions (PBC) and Particle Mesh Ewalds (PME) methods were utilized for treating the long-range electrostatic interactions. The non-bonded cut-off radius was set as 10 Å for the nonbonding (Lennard-Jones (LJ 6-12) and Coulomb) interactions. Water molecules around the CA IX were equilibrated with 500 ps MD simulations at fixed coordinates of the atoms of the CA IX. The production MD run was then carried out for 10 ns for all the studied system (Figure 2) without any constraints.

Co-crystallized ligand docking

In an initial step, we tested the capability of Glide/induced fit docking (IFD)²⁹, Glide/SP and Glide/XP³⁰ protocols to predict the ligand position of reference ligand (Figure 1) in the CA IX X-ray structure. Co-crystallized inhibitor is used at the ligand preparation module LigPrep³¹ and then it is docked into the active site of the protein using the Glide docking protocols with different approaches. The binding cavity was assigned as an outer box of $(30 \times 30 \times 30) \text{ \AA}^3$ which is determined by the position of the reference ligand. We employed the SP, XP and IFD methods of the Glide docking. The conformation of co-crystallized X-ray structure is compared with docking poses. RMSD values for all used docking methods were found as less than 1.5 Å (Figure 3).

Virtual docking screening

It has become possible to perform HTVS on large libraries (i.e. ZINC database) with the enormous increase in computer facilities. Chemical structures of around 7 million ligands are

obtained from the ZINC database in the present study³². The 3D structures were prepared using LigPrep module of Maestro. The physiological medium and ionization states were determined for all the ligands and the pH was set to 7.4. The docking screening process was carried out in two steps: (i) Glide/HTVS is performed for accelerated docking simulations of 7 million ligands, (ii) the ligands with top-docking scores from HTVS were selected for further detailed analyses by Glide/XP docking.

ADME analysis

The absorption, distribution, metabolism and excretion (ADME) characteristics of all selected compounds were predicted using QikProp³³ software, which calculates physicochemical properties of the compounds. This software may validate the drug-likeness of the ligands based on Lipinski's criteria³⁴.

In vitro analysis

Adherent epithelium renal cell adenocarcinoma cell line (ACHN, ATCC CRL-1611) was grown at Dulbecco's modified Eagle's medium (Sigma-Aldrich, Germany) containing 10% (v/v) FBS, 100 units/mL streptomycin and 100 µg/mL penicillin. Cells were maintained 80% confluency at 5% CO_2 at 37 °C into T75 flasks and then transferred into four T125 flask and maintained 90% confluency. Cells were quickly washed three times with 50 mM K_xPO_4 buffer. Cells were scratched from T125 flasks and transferred into falcon tubes (4 °C) and centrifuged 1500 rpm, 4 °C, 5 min. The cell pellet was maintained at -80 °C for 4 h and then lyophilized. About 1 mL dry ACHN cell pellet was obtained. CA IX activity was assayed by following the change in absorbance at 348 nm of 4-nitrophenylacetate (NPA) to 4-nitrophenylate ion over a period of 3 min at 25 °C using a spectrophotometer (Shimadzu UV-VIS) according to the method described by Verpoorte et al.³⁵ The enzymatic reaction, in a total volume of 3.0 mL, contained 1.4 mL 0.05 M tris-SO₄ buffer (pH 7.4), 1.0 mL 3 mM NPA, 0.5 mL H₂O and 0.1 mL enzyme solution. A reference measurement was obtained by preparing the same cuvette without enzyme solution. The Lineweaver–Burk curves were used to determine kinetic parameters and inhibition constants³⁶.

Results and discussions

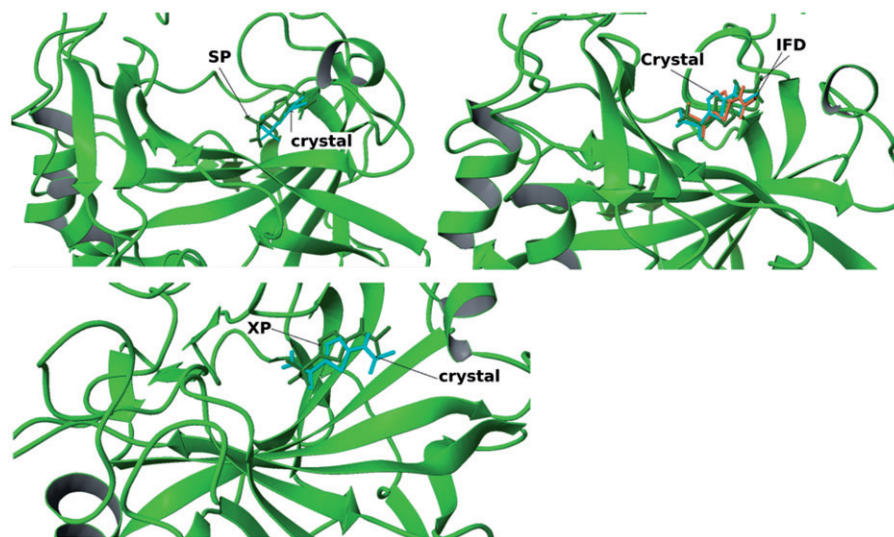
MD simulations

It is necessary to prepare the used X-ray structure and to relax the target before starting the drug screening in order to get successful results. For this aim, we performed 10 ns MD simulations to relax the CA IX complex. Figure S1 shows the RMSD of the $C\alpha$ atoms of the target during the MD stimulations. It is clear that system reached to the acceptable stability after the 3.0 ns simulations. Average structure from generated trajectories is constructed and representative structure selected from the derived trajectories, which is the smallest RMSD with the average structure, for docking simulations.

Structure-based virtual screening

The ZINC ligand library consists of commercially available ligand structures for docking screening. It involves almost 20 million ligands that can be used for virtual screening. In order to determine novel CA-IX inhibitors from the ZINC database, Glide/HTVS docking simulations for 7 million drug-like ligands were performed. Out of these ligands, 70 compounds were selected with the high-binding scores at the target site (see supplementary Figure S2). Glide/XP protocol is then utilized to identify the final CA-IX inhibitor candidates. Their chemical structures and

Figure 3. Cognate docking poses alignment with the co-crystallized ligand conformation using different methods.



binding energies are shown in Table 1. There are two criteria for choosing the potent ligands. The screened ligands were ranked according to their docking scores and ligands forming critical hydrogen bonding interactions with key-residues such as Thr199 and Thr200 at active sites are also considered. All the reported selected compounds have docking scores of less than -8 kcal/mole (Table 1). In order to better understand the molecular mechanisms of inhibition profiles of the selected CA IX inhibitors, their docking poses at the binding site are analyzed (Figure S3). Figure S3 shows the ligand interaction diagram for each selected compound at the binding pocket of CA IX. All selected ligands were superimposed in the active pocket in order to show the population of the ligand poses (Figure 4). As it is shown, functional groups of similar chemical properties were positioned in similar modes with analogous bindings with the CA IX residues and encourage for an acceptable protein–ligand interactions, that was indicated the same inhibitory treatment of these ligands (Figure 4). The docked poses of selected ligands display reasonable hydrogen-bonding network including the hydroxyl group in most of the selected compounds and polar residue of the active cavity.

The top docking pose of compound from the ZINC database (ZINC20464003) was shown in Figure 5. This ligand fits into the CA IX active cavity. The ligand–protein complex was stabilized by establishing four polar interactions via residues Asn62, Gln67, Thr199 and Thr200 at the target. The other main residues that participated in hydrophobic interactions were represented as 2D ligand interaction diagram using docking poses of ZINC20464003 and ZINC72421916 compounds in Figure 5. Thr200, His94 and Thr199 were suggested as key amino acid residues in CA IX inhibitory mechanism¹⁹. All these amino acids formed strong interactions with docked compounds in our study.

Physicochemical predictions of docked compounds

ADME analysis was also performed for the selected compounds. Physicochemical and pharmaceutical properties of selected ligands which involve molecular weight, octanol/water partition coefficient, apparent Caco-2 cell permeability in nm/s, blockage of hERG K channel, percentage of human oral absorption and Lipinski's rule of five were listed in Table 2. As shown, all of the predicted values are in the acceptable ranges. Lipinski's rule of 5 is a rule of thumb to predict drug like compounds and, selected compounds were positioned in good range of Lipinski's rule.

In addition, a similarity search toward standard drugs was carried out. All the discovered ligands displayed more than 80% similarity towards known drugs are listed in Table S1. As shown in Table S1, beta-adrenergic antagonists (Propranolol, Timolol, Nebivolol, Tretolol, Carazolol, Bucumolol, Tertatolol, Penbutolol and Xamoterol) have more similarity with proposed selected compounds in this study. It is known that beta-adrenergic inhibitors block the carbonic anhydrase receptors³⁷. These experimental reports can validate the results of present virtual screening study. In order to compare docking scores of known CA-IX inhibitors with selected compounds from our study, we docked 14 known CA-IX inhibitors^{38–44} at the active site of the target. Docking scores and chemical structures of these compounds are found in the range of -5.66 to -6.79 kcal/mole (Table S2).

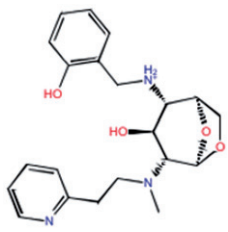
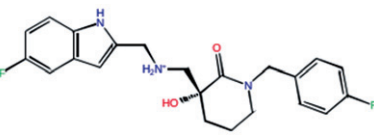
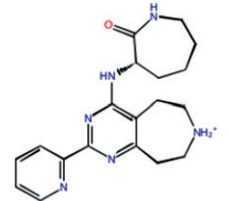
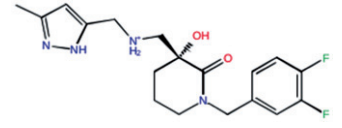
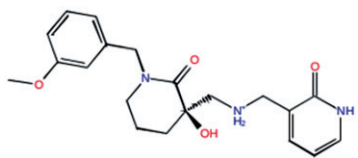
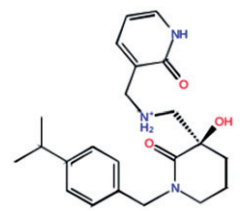
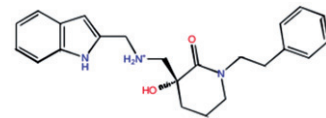
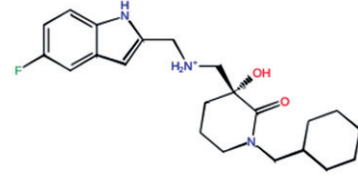
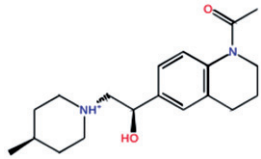
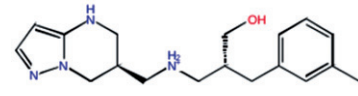
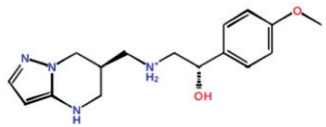
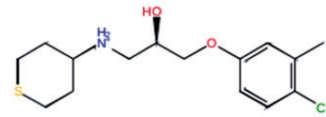
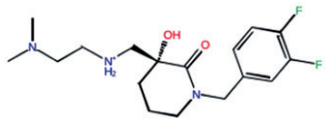
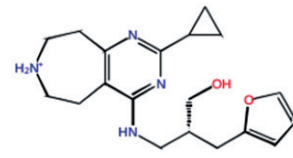
In vitro analysis

In order to test and validate the predicted results of molecular simulations three compounds are ordered from available compound databanks (ChemBridge Corporation, San Diego, CA) and tested by *in vitro* analysis. Results showed that all compounds are inhibited CA IX in the range of 0.85 – 1.58 μM K_i values. Interestingly docking scores of these compounds are in correct order with their inhibition data (Table 3). 3D docking poses and 2D ligand interaction diagrams of these selected compounds are represented in Figures 6 and 7.

Conclusions

We performed a low-cost and accelerated structure-based virtual screening method^{45–48} to discover novel inhibitor candidates of hCA IX. In summary, ~ 7 million compounds from the ZINC database were virtually screened against CA IX to discover novel ligands with high affinity toward this target. 70 ligands showed a high-docking score using Glide/HTVS method. These compounds are then docked with Glide/XP method and 19 of them showed high-docking scores at the binding cavities of the CA IX target. All selected compounds displayed drug-like properties and their properties are similar to standard drugs. A few of these ligands are ordered from available provider of the ligands and tested by *in vitro* analysis in order to validate the molecular simulations results. *In vitro* analysis showed that ZINC67714195, ZINC11935360, and ZINC67458868 compounds inhibited hCA IX by K_i values of 0.85 , 1.03 , and 1.58 μM , respectively. These

Table 1. 2D chemical structures and their corresponding docking scores for selected top-docking scored compounds.

Compound	Chemical structures	Glide/XP scores (kcal/mole)	Compound	Chemical structures	Glide/XP scores (kcal/mole)
ZINC20464003		-9.80	ZINC67956012		-9.42
ZINC72421916		-9.66	ZINC11935360		-9.41
ZINC67805921		-9.47	ZINC67433231		-9.30
ZINC01592824		-9.45	ZINC67433435		-9.10
ZINC67714195		-9.43	ZINC67458868		-8.69
ZINC12291144		-8.67	ZINC58328414		-8.30
ZINC58327836		-8.61	ZINC32533143		-8.22
ZINC67850016		-8.38	ZINC72438236		-8.22

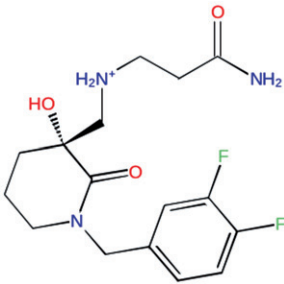
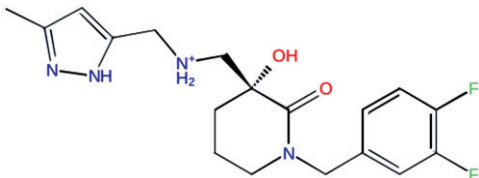
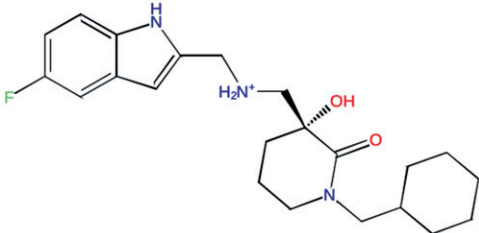
(continued)

Table 2. Selected compounds with their ADME properties.

Compound	mol MW ^a	QplogP o/w ^b	QPPCaco ^c	QplogHERG ^d	Percent human oral absorption ^e	Rule of five
ZINC20464003	385.46	0.61	68.54	−6.02	63.39	+
ZINC72421916	352.44	1.60	128.29	−4.21	74.04	+
ZINC67805921	371.44	1.89	318.28	−4.73	82.83	+
ZINC01592824	215.18	−2.30	3.43	−2.04	23.04	+
ZINC67714195	341.36	0.58	44.33	−2.64	59.83	+
ZINC67956012	399.44	4.13	678.67	−4.83	100.00	+
ZINC11935360	364.39	2.82	302.50	−4.54	87.86	+
ZINC67433231	383.49	2.68	354.23	−4.51	88.25	+
ZINC67433435	377.49	3.58	263.38	−4.95	91.20	+
ZINC67458868	387.50	4.11	873.75	−4.35	100.00	+
ZINC12291144	316.44	2.37	398.16	−5.12	87.34	+
ZINC58327836	302.38	2.08	290.27	−5.62	83.22	+
ZINC67850016	341.40	2.15	227.63	−4.79	81.70	+
ZINC40528234	282.77	0.40	74.90	−3.57	62.86	+
ZINC58328414	314.43	2.69	263.47	−5.18	86.00	+
ZINC32533143	315.86	3.03	671.66	−4.84	95.31	+
ZINC72438236	342.44	2.53	351.71	−5.20	87.35	+

^aMolecular weight (reasonable value <500).^bPredicted octanol/water partition coefficient (reasonable value from −2.0 to 6.5).^cPredicted apparent Caco-2 cell permeability in nm/s (reasonable value >25).^dPredicted blockage of hERG K⁺ channel (reasonable value <−7).^ePercentage of human oral absorption (<25% is weak and >80% is strong).

Table 3. hCA IX inhibition data of selected compounds.

Compound	Chemical structures	Determined K _i (μM)* hCA IX	Predicted K _i (μM)** hCA IX
ZINC67714195		0.85	0.227
ZINC11935360		1.03	0.231
ZINC67458868		1.58	0.750

*Mean from at least three determinations. Errors in the range of 1–3% of the reported value (data not shown).

**Converted from top-docking scores.

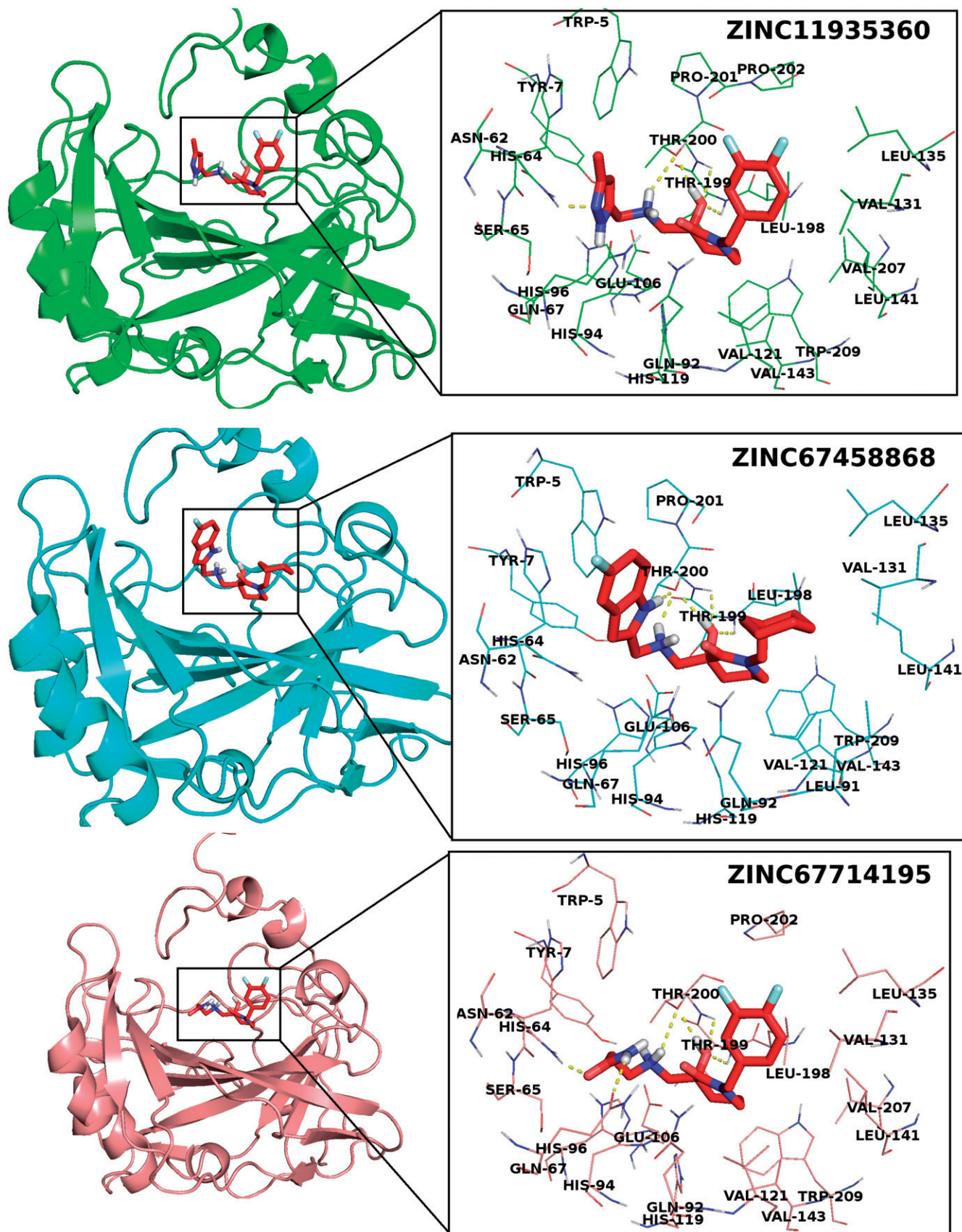


Figure 6. 3D docking poses of selected compounds at the active site of CA-IX.

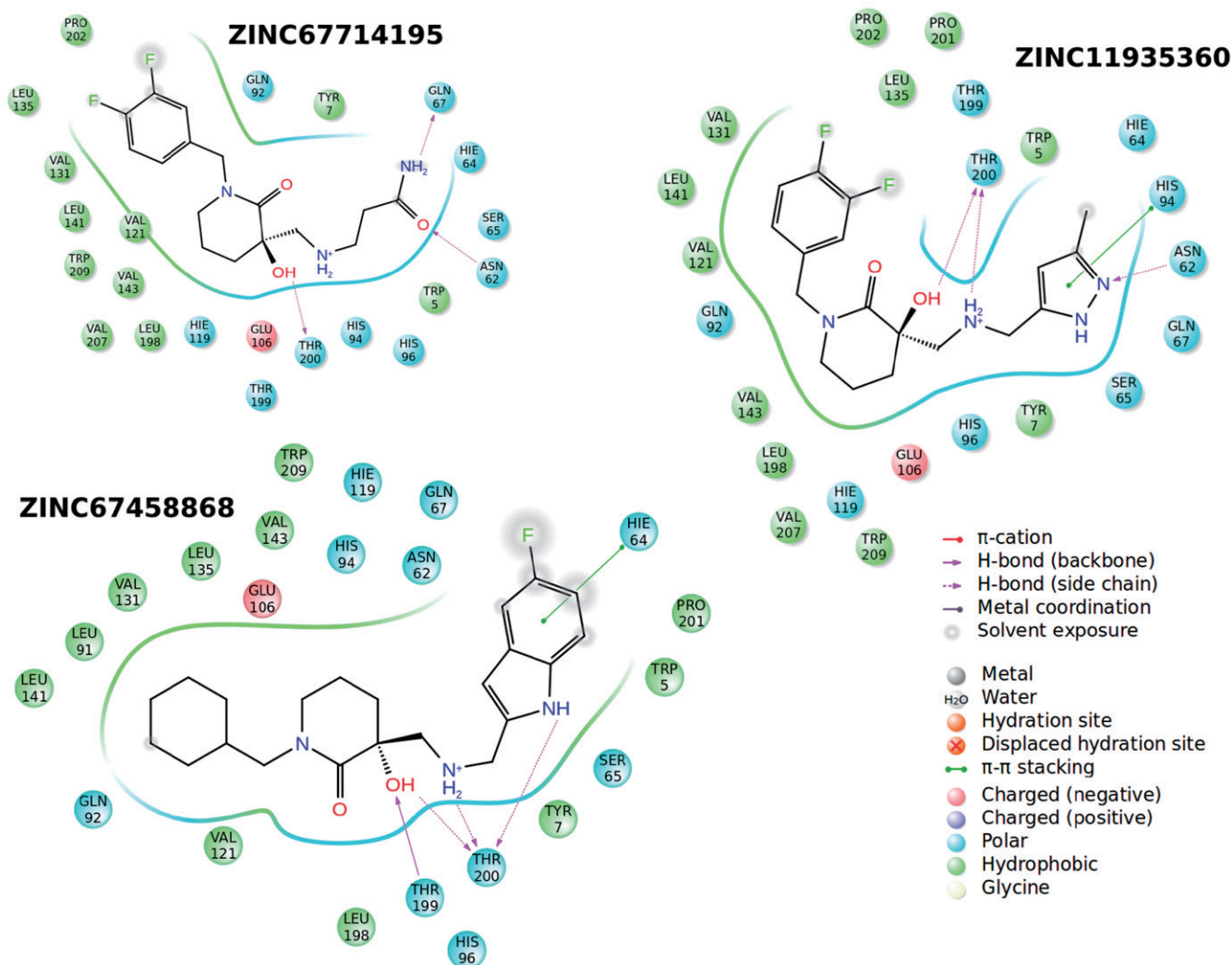


Figure 7. 2D ligand interaction diagrams of selected compounds into the active site of CA-IX.

discovered novel compounds may be guided as candidate inhibitors of CA IX.

Acknowledgments

Part of computations for the work described in this paper was supported by Turkish Scientific and Technical Research Council (TUBITAK) ULAKBIM High Performance Computing Center. SD acknowledges support from Bilim Akademisi - The Science Academy, Turkey, under the BAGEP program

Declaration of interest

The authors report no conflicts of interest. The authors alone are responsible for the content and writing of this article.

References

1. Thiry A, Dogné JM, Masereel B, Supuran CT. Targeting tumor-associated carbonic anhydrase IX in cancer therapy. *Trends Pharmacol Sci* 2006;27:566–73.
2. Pastorek J, Pastoreková S, Callebaut I, et al. Cloning and characterization of MN, a human tumor-associated protein with a domain homologous to carbonic anhydrase and a putative helix-loop-helix DNA binding segment. *Oncogene* 1994;9:2877–88.
3. Balaydin HT, Durdagi S, Ekinci D, et al. Inhibition of human carbonic anhydrase isozymes I, II and VI with a series of bisphenol, methoxy and bromophenol compounds. *J Enzyme Inhib Med Chem* 2012;27:467–75.
4. Ekinci D, Kurbanoglu NI, Salamci E, et al. Carbonic anhydrase inhibitors: inhibition of human and bovine isoenzymes by benzenesulphonamides, cyclitols and phenolic compounds. *J Enzyme Inhib Med Chem* 2012;27:845–8.
5. Ekinci D, Al-Rashida M, Abbas G, et al. Chromone containing sulfonamides as potent carbonic anhydrase inhibitors. *J Enzyme Inhib Med Chem* 2012;27:744–7.
6. Cavdar H, Ekinci D, Talaz O, et al. alpha-Carbonic anhydrases are sulfatases with cyclic diol monosulfate esters. *J Enzyme Inhib Med Chem* 2012;27:148–54.
7. Senturk M, Ekinci D, Goksu S, Supuran CT. Effects of dopaminergic compounds on carbonic anhydrase isozymes I, II, and VI. *J Enzyme Inhib Med Chem* 2012;27:365–9.
8. Ekinci D, Karagoz L, Ekinci D, et al. Carbonic anhydrase inhibitors: in vitro inhibition of α isoforms (hCA I, hCA II, bCA III, hCA IV) by flavonoids. *J Enzyme Inhib Med Chem* 2013;28: 283–8.
9. Ozdemir ZO, Senturk M, Ekinci D. Inhibition of mammalian carbonic anhydrase isoforms I, II and VI with thiamine and thiamine-like molecules. *J Enzyme Inhib Med Chem* 2013;28: 316–19.
10. Abdel-Aziz AA-M, El-Azab AS, Ekinci D, et al. Investigation of arenesulfonyl-2-imidazolidinones as potent carbonic anhydrase inhibitors. *J Enzyme Inhib Med Chem* 2015;30:81–4.
11. Korkmaz N, Obaidi OA, Senturk M, et al. Synthesis and biological activity of novel thiourea derivatives as carbonic anhydrase inhibitors. *J Enzyme Inhib Med Chem* 2015;30:75–80.

12. Pastorekova S, Parkkila S, Zavada J. Tumor-associated carbonic anhydrases and their clinical significance. *Adv Clin Chem* 2006;42:167–216.
13. Wykoff CC, Beasley NJP, Watson PH, et al. Hypoxia-inducible expression of tumor-associated carbonic anhydrases. *Cancer Res* 2000;60:7075–83.
14. Potter C, Harris AL. Hypoxia inducible carbonic anhydrase IX, marker of tumor hypoxia, survival pathway and therapy target. *Cell Cycle* 2004;3:164–7.
15. Supuran CT, Scozzafava A, Casini A. Carbonic anhydrase inhibitors. *Med Res Rev* 2003;23:146–89.
16. Swietach P, Wigfield S, Cobden P, et al. Tumor-associated carbonic anhydrase 9 spatially coordinates intracellular pH in three-dimensional multicellular growths. *J Biol Chem* 2008;283:20473–83.
17. Supuran CT. Carbonic anhydrases: novel therapeutic applications for inhibitors and activators. *Nat Rev Drug Discov* 2008;7:168–81.
18. Supuran CT. Carbonic anhydrases as drug targets – an overview. *Curr Top Med Chem* 2007;7:825–33.
19. Alterio V, Hilvo M, Di Fiore A, et al. Crystal structure of the catalytic domain of the tumor-associated human carbonic anhydrase IX. *Proc Natl Acad Sci USA* 2009;106:16233–8.
20. Berman HM, Westbrook J, Feng Z, et al. The Protein Data Bank. *Nucleic Acids Res* 2000;28:235–42.
21. (a) Schrödinger Suite 2012 Protein Preparation Wizard; Epik version 2.3. New York (NY): Schrödinger, LLC; 2012. (b) Impact version 5.8. New York (NY): Schrödinger, LLC; 2012. (c) Prime version 3.1. New York (NY): Schrödinger, LLC; 2012.
22. Mårtensson L-G, Karlsson M, Carlsson U. Dramatic stabilization of the native state of human carbonic anhydrase II by an engineered disulfide bond. *Biochemistry* 2002;41:15867–75.
23. Li H, Robertson AD, Jensen JH. Very fast empirical prediction and rationalization of protein pK_a values. *Proteins Struct Funct Genet* 2005;61:704–21.
24. Bas DC, Rogers DM, Jensen JH. Very fast prediction and rationalization of pK_a values for protein-ligand complexes. *Proteins Struct Funct Genet* 2008;73:765–83.
25. Olsson MHM, SØndergaard CR, Rostkowski M, Jensen JH. PROPKA3: Consistent treatment of internal and surface residues in empirical pK_a predictions. *J Chem Theory Comput* 2011;7:525–37.
26. Humphrey W, Dalke A, Schulten K. VMD: Visual molecular dynamics. *J Mol Graph* 1996;14:33–8.
27. Phillips JC, Braun R, Wang W, et al. Scalable molecular dynamics with NAMD. *J Comput Chem* 2005;26:1781–802.
28. Zhu X, Lopes PEM, Mackerell AD. Recent developments and applications of the CHARMM force fields. *Wiley Interdisciplinary Rev* 2012;2:167–85.
29. Friesner RA, Banks JL, Murphy RB, et al. Glide: a new approach for rapid, accurate docking and scoring. 1. Method and assessment of docking accuracy. *J Med Chem* 2004;47:1739–49.
30. Suite 2012: Glide, version 5.8. New York (NY): Schrödinger, LLC; 2012.
31. Suite 2012: LigPrep, version 2.5. New York (NY): Schrödinger, LLC; 2012.
32. Irwin JJ, Shoichet BK. ZINC – a free database of commercially available compounds for virtual screening. *J Chem Inf Model* 2005;45:177–82.
33. QikProp, version 3.5. New York (NY): Schrödinger, LLC; 2012.
34. Lipinski CA, Lombardo F, Dominy BW, Feeney PJ. Experimental and computational approaches to estimate solubility and permeability in drug discovery and development settings. *Adv Drug Deliv Rev* 2001;46:3–26.
35. Verpoorte JA, Mehta S, Edsall JT. Esterase activities of human carbonic anhydrases B and C. *J Biol Chem* 1967;242:4221–9.
36. Lineweaver H, Burk D. The determination of enzyme dissociation constants. *J Am Chem Soc* 1934;56:658–66.
37. Puşcas I, Reznicek A, Moldovan A, et al. Activation of carbonic anhydrase by beta-adrenergic agonists and inhibition by beta-adrenergic blockers. *Med Interne* 1985;23:185–9.
38. Turkmen H, Durgun M, Yilmaztekin S, et al. Carbonic anhydrase inhibitors. Novel sulfanilamide/acetazolamide derivatives obtained by the tail approach and their interaction with the cytosolic isozymes I and II, and the tumor-associated isozyme IX. *Bioorganic Med Chem Lett* 2005;15:367–72.
39. Maresca A, Temperini C, Pochet L, et al. Deciphering the mechanism of carbonic anhydrase inhibition with coumarins and thiocoumarins. *J Med Chem* 2010;53:335–44.
40. Innocenti A, Gülçin I, Scozzafava A, Supuran CT. Carbonic anhydrase inhibitors. Antioxidant polyphenols effectively inhibit mammalian isoforms I–XV. *Bioorganic Med Chem Lett* 2010;20:5050–3.
41. Winum JY, Pastorekova S, Jakubickova L, et al. Carbonic anhydrase inhibitors: synthesis and inhibition of cytosolic/tumor-associated carbonic anhydrase isozymes I, II, and IX with bis-sulfamates. *Bioorganic Med Chem Lett* 2005;15:579–84.
42. Winum JY, Innocenti A, Scozzafava A, et al. Carbonic anhydrase inhibitors. Inhibition of the human cytosolic isoforms I and II and transmembrane, tumor-associated isoforms IX and XII with boronic acids. *Bioorganic Med Chem* 2009;17:3649–52.
43. Durdagi S, Sentürk M, Ekinci D, et al. Kinetic and docking studies of phenol-based inhibitors of carbonic anhydrase isoforms I, II, IX and XII evidence a new binding mode within the enzyme active site. *Bioorganic Med Chem* 2011;19:1381–9.
44. Pacchiano F, Carta F, McDonald PC, et al. Ureido-substituted benzenesulfonamides potently inhibit carbonic anhydrase IX and show antimetastatic activity in a model of breast cancer metastasis. *J Med Chem* 2011;54:1896–902.
45. Mavromoustakos T, Durdagi S, Koukoulitsa C, et al. Strategies in the rational drug design. *Curr Med Chem* 2011;18:2517–30.
46. Politi A, Durdagi S, Moutevelis-Minakakis P, et al. Development of accurate binding affinity predictions of novel renin inhibitors through molecular docking studies. *J Mol Graph Model* 2010;29:425–35.
47. Durdagi S, Scozzafava GL, Vullo D, et al. Inhibition of mammalian carbonic anhydrases IXIV grayanotoxin III: solution and in silico studies. *J Enzyme Inhib Med Chem* 2013;29:469–75.
48. Ekinci D, Fidan I, Durdagi S, et al. Kinetic and in silico analysis of thiazolidin-based inhibitors of α -carbonic anhydrase isoenzymes. *J Enzyme Inhib Med Chem* 2013;28:370–4.